Table 2 Critical pressures for cylinder for different boundary conditions

Type of boundary condition	Critical pressure	
	n	λ_{cr}
Eq. (5a)	5	0.0371
	6	0.04192
Eq. (5b)	5	0.03985
	6	0.0464
Eq. (5c)	5	0.04555
	6	0.04937
Eq. (5d)	5	0.05203
	6	0.05465

values of $\bar{Z}_0$, the shell buckles into more number of circumferential waves, if membrane prebuckling is employed.

Effect of Buckling Boundary Conditions

The possible set of simply-supported boundary conditions are

$$W_n^* = M_{sn}^* = N_{sn}^* = N_{s\theta n}^* = 0 \tag{5a}$$

$$W_n^* = M_{sn}^* = N_{sn}^* = V_n^* = 0 \tag{5b}$$

$$W_n^* = M_{sn}^* = U_n^* = N_{s\theta n}^* = 0 \tag{5c}$$

$$W_n^* = M_{sn}^* = U_n^* = V_n^* = 0 \tag{5d}$$

For the previously listed boundary conditions, critical loads of a shell whose thickness variation corresponds to S. No. 1 of Table 1 are given in Table 2. A shell whose inplane displacements are restrained completely, buckles at higher pressures than a shell having zero inplane edge forces. Critical pressures for the other two boundary conditions fall within the aforementioned limits.

Conclusions

The numerical results presented here show that shells of variable thickness having particular thickness variation resists higher lateral pressures than shells of constant (average) thickness for an assumed set of boundary conditions. Critical pressures of short shells, based on consistent prebuckling analysis, are larger than membrane analysis.

References

[1] Federhofer, K., "Stabilitat Der Krieszylinderschale Mit Veranderlicher Wandstarke," *Osterreichisches*, Ingenieur—Archiv, Vol. 6, 1952, pp. 277-288.

[2] Wagner, H., "Die Stabilitat Der Axial Gendruckten Kreiszylinderschale Mit Veranderlicher Wandstarke," *Osterreichischers*, Ingenieur-Archiv, Vol. 13, 1959, pp. 235-257.

[3] Ross, C. T. F., "Elastic Instability of a Circular Cylinder of Varying Shell Thickness," *Quarterly Transactions of Royal Society for Naval Architects*, Vol. 110, April 1968, pp. 247-290.

[4] Sanders, J.L. "Nonlinear Theories for Thin Shells," *Quarterly of Applied Mathematics*, Vol. 21, April 1963, pp. 21-36.

[5] Radhamohan, S. K., "Nonlinear Stability of Thin Shells of Revolution by Parametric Differentiation Technique," Ph. D. thesis, 1971, Dept. of Civil Engineering, Indian Institute of Technology, Kanpur, India.

[6] Radhamohan, S. K. and Prasad, B., "Axymmetric Buckling of Toroidal Shells under Axial Tension," *AIAA Journal*, Vol. 12, April 1974, pp. 511-515.

[7] Batdorf, S. B., "A Simplified Method of Elastic Stability Analysis for Thin Cylindrical Shells—I—Donnell's Equations," June 1947, NACA TN-1341.

Debris Shielding in Regions of High Edge Velocity

David H. Smith*
Prototype Development Associates, Inc., Santa Ana, Calif.

Nomenclature

A	= area, ft^2
B	= mass loss constant, sec^2/ft^2
C	= trajectory constant, 1/ft
C_D	= drag coefficient
D	= particle diameter, ft
e	= base of natural logarithms
G	= ratio of eroded-to-impact mass,
m	= mass, lb
$\dot{m}$	= incident mass flux, lb/ft^2-sec
$P(n)$	= probability of n collisions
r	= radius, ft
s	= running length, ft
t	= time, sec
V	= velocity, ft/sec
ρ	= density, lb/ft^3
θ	= angle from velocity vector ($\theta_{stag} = 90$), degree
Subscripts	
b	= body
d	= debris
e	= boundary-layer edge
I	= impact
o	= original
p	= particle
rel	= relative

Introduction

IT has been established,[1] that for sufficiently high particle fluxes, 1) the erosion of the stagnation region of a blunt body traversing a particle cloud at hypersonic velocity is a nonlinear function of the particle impacting mass flux, and 2) this nonlinearity can be explained by debris shielding. Some incoming particles will collide with debris fragments created by upstream collisions. Due to the large difference in velocity between the particle and debris fragment, these collisions reduce the surface impact damage and, in effect, "shield" the surface. The majority of the work on debris shielding to date has been for stagnation regions. This note attempts to extend debris shielding analysis to regions with super-or hypersonic edge velocity.

The probability of debris-particle collisions and the resultant damage are studied for regions of high edge velocity. It is shown that in such regions debris shielding for typical reentry conditions is dominated by debris created only a few inches upstream of any point under analysis.

Analytical Methods

The computer program used for this analysis calculates ablation, erosion, and shape change for hypersonic vehicles. Flow parameters are calculated by a streamwise numerical integration so that the effects of the bow-shock-generated entropy layer are accounted for by a streamtube mass balance. In the erosion calculations[2] particle trajectories are calculated from the shock to the body by coupling the effects of

Received February 18, 1975; revision received June 6, 1975. This work was sponsored by the Defense Nuclear Agency under contract, DNA 001-75-C-0054.

Index categories: Multiphase Flows; Hypervelocity Impact.

*Engineering Associate.

deceleration, deflection, and mass loss. Two mechanisms are considered that reduce some of the particle mass into droplets small enough to follow streamlines and miss the body: 1) shattering and droplet stripping for liquid drops, and 2) melting with simultaneous droplet stripping for frozen particles. Debris shielding based on the mass of debris intercepted by an incoming particle is determined. To determine this mass for a particle impacting one segment of the vehicle, it is necessary to determine the distributions and velocities of the debris fragments from each upstream segment as they pass over the impacted segment.

To determine the distributions, it is assumed that each particle impact produces a hemispherical bubble of debris (Fig. 1), on the surface of which the debris is distributed uniformly and moves radially at a velocity obtained from conservation of momentum

$$V_{do} = V_{pI}/G \tag{1}$$

It is assumed that this radial velocity is constant and much less than the gas velocity, and that the bubble radius is always much less than the local body radius.

To determine the mean velocity of the debris bubble, the following expressions for the streamwise position and velocity of a debris bubble were derived by integrating the equation for aerodynamic acceleration. In this derivation, it was assumed that the fragments have constant unity drag coefficients, and that the gaseous boundary layer and interactions among debris fragments were negligible

$$s = V_e t - \ell n[(V_e - V_o)Ct + 1)]/C$$

$$V_d = V_e - (V_e - V_o)/[(V_e - V_o)Ct + 1]$$

$$C = \rho_e C_D A_d / 2m_d = 0.75\rho_e/(D_d \rho_d) \tag{2}$$

These equations are integrated numerically along the body, assuming a mean streamwise velocity of zero at the point of origin. The radius of the debris bubble above the k^{th} segment of debris fragments from the jth segment is then

$$r_{djk} = V_{od}(t - t_I) \tag{3}$$

The mass intercepted by an incoming particle that collides with the bubble is approximated by

$$m_{djk} = G m_{plj}(r_{pI}^2/2r_{djk}^2) \tag{4}$$

Assuming that the debris bubbles cover only a fraction of the surface area of the body at any instant, the probability of encountering no debris at all must be determined. The average obscuration of the k^{th} body segment by debris bubbles from the j^{th} segment is

$$\text{OBSC}_{jk} = (\text{traversal time})\,(\text{creation rate})$$

$$(\text{bubble area/segment area})$$

$$= \Delta t_{jk}(\dot{m}_{Ij}/m_{plj})\ (\pi r_{djk}^2/A_k) \tag{5}$$

This obscuration represents the average number of debris bubbles from the j^{th} segment with which a particle impacting the kth segment collides. Due to the debris noninteraction assumption, the average total number of debris bubble collisions experienced by the particle impacting the kth segment is simply

$$\text{OBSC}_k = \sum_{j=1}^{k} \text{OBSC}_{jk} \tag{6}$$

It can be shown from basic probability theory that the probabilities of a particle impacting the kth body segment without colliding with any bubbles from the jth segment or any bubbles from any segment are, respectively

$$P(0)_{jk} = (1/e)^{\text{OBSC}_{jk}} \qquad P(0)_k = (1/e)^{\text{OBSC}_k}$$

Collisions with debris are expected to break up mechanically-weak particles, such as water droplets and ice crystals. The resultant smaller fragments would experience higher aerodynamic deceleration, thus reducing the kinetic energy transferred to the body at impact. In the following analysis, this fragmentation is treated as a loss in particle effective mass and is assumed to be proportional to the kinetic energy associated with the debris-particle collision

$$\Delta m_{pjk} = B m_{djk} V_{rel}^2 \tag{7}$$

$$V_{rel} = (V_{x\,rel}^2 + V_{y\,rel}^2)^{1/2} \tag{8}$$

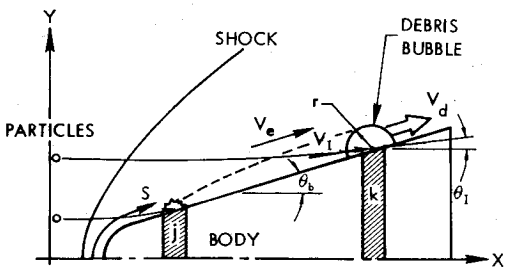

Fig. 1 Geometry.

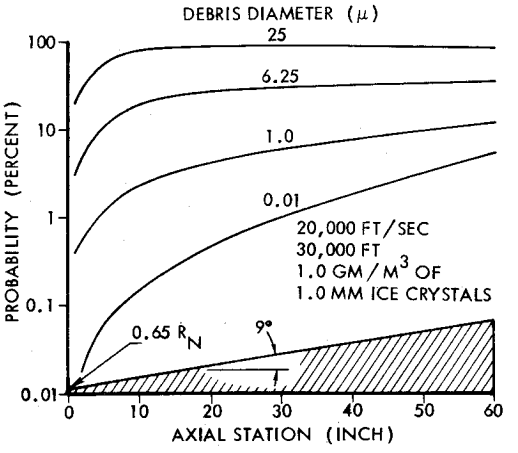

Fig. 2 Probability of at least one debris particle collision (1.0 gm/m³).

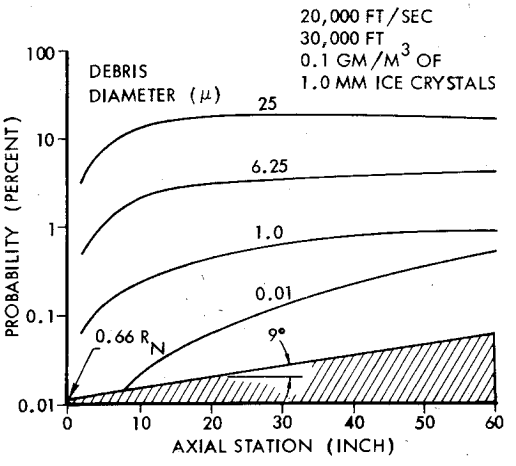

Fig. 3 Probability of at least one debris particle collision (0.1 gm/m³).

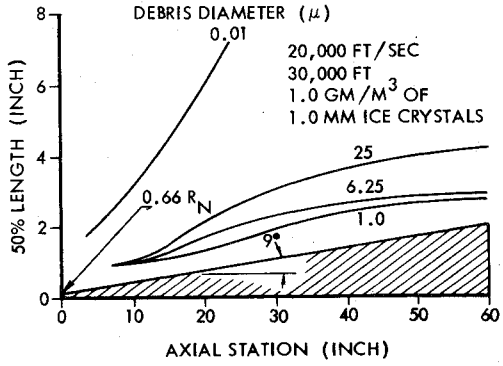

Fig. 4 50% length distributions.

$$V_{x\,rel} = V_I \cos\theta_p - V_d \cos\theta_b \tag{9}$$

$$V_{y\,rel} = V_I \sin\theta_p - V_d \sin\theta_b \tag{10}$$

Neglecting particle cross-section area change and the probability of colliding with more than one bubble from any single segment, the average mass of a particle impacting the *kth* segment is

$$m_{pIk} = m_{pok} - \sum_{j=1}^{k} (1 - P(0)_{jk})\,\Delta m_{pjk} \tag{11}$$

Results

A typical re-entry vehicle and particle environment were analyzed. Debris fragment diameters from 0.01 to 25 μ and cloud densities from 0.1 to 1.0 gm/m^3 were studied. Figures 2 and 3 show the probability of a particle encountering debris fragments from any upstream segment (e.g., unity minus the probability shown is the probability that a particle would encounter no debris fragments).

The results of the particle mass loss calculations for the previous cases indicate that debris shielding at any point on the body is dominated by debris generated immediately upstream from that point. To provide a more convenient parameter for studying the upstream extent of the region providing significant shielding of a point, the "50% length" is defined as the upstream extent of the segment that produces 50% of the debris shielding of that point. Figure 4 shows the variation in 50% length along a re-entry vehicle for debris fragments sizes from 0.01 to 25 microns. Since heatshields are reinforced typically with filaments that are on the order of 10 μ in diameter, it would be expected that a large fraction of the debris would be in that size class. Since Fig. 4 shows that for fragments larger than 1.0 μ the 50% length never exceeds 4 in., it appears that debris shielding is dominated by slow-moving debris fragments. This is analogous to the stagnation region debris shielding and implies that stagnation point shielding correlations might be applicable to heatshields also.

The previous analysis was repeated assuming that the debris fragments from each upstream body segment were distributed uniformly in the debris layer rather than being confined to discrete bubbles. Interestingly, the 50% length predictions vary little from those shown above.

References

[1] Reinecke, W.G., "Debris Shielding During High-Speed Erosion," *AIAA Journal*, Vol. 12, Nov. 1974, pp. 1592-1594.

[2] Smith, D.H., "A Computer Analysis of Shock Layer/Particle Interactions," PDA Rept. TB 4001-00-01, 15 April 1974, Prototype Development Associates, Inc., Santa Ana, Calif.

Viscous Flow Around Close-Fitting Spherical Pistons in Right Circular Cylinders

G. David Huffman*
Indianapolis Center for Advanced Research and Indiana-Purdue University at Indianapolis, Ind.

Introduction

HYDRAULIC actuators, pumps and motors, and hydrostatic transmissions which are utilized in both air and ground transportation systems can be reduced in cost by using a small-clearance spherically ground piston within a right circular cylinder. The use of this concept eliminates the need for a wrist-pin and intricate sealing mechanisms resulting in decreased costs. To obtain maximum efficiency from these units, it will be necessary to provide a piston-cylinder clearance which will limit the leakage losses past the piston due to the pressure differential without incurring excessive torque loss from viscous shear forces and mechanical friction. The purpose of this Note is to both predict and measure the leakage flow and frictional characteristics of spherical pistons in close fitting cylinders as a function of imposed pressure difference, piston velocity, clearance, eccentricity, and fluid viscosity.

Experimental Apparatus

The experimental program was carried out in two phases. The first phase consisted of determining the flow past a close fitting spherical piston in a cylinder subjected to an imposed pressure difference. This experiment is similar to Poiseuille[1] flow in that both the piston and cylinder were fixed and a pressure differential applied. The objective of the second experiment was to determine the viscous shear and mechanical frictional forces encountered when the close-fitting spherical piston moves at high speeds within the cylinder. This phase is analogous to Couette[1] flow wherein the piston is moved at constant velocity and no external pressure differential is imposed.

In an actual application both of the previous processes occur simultaneously. The two conditions are dealt with separately in the experimental program in order to simplify the apparatus. The two effects are combined theoretically using a mathematical model developed in this Note.

A test apparatus was fabricated to measure oil leakage past the piston as shown in Fig. 1. Test cylinders and test pistons of different diameters were manufactured to cover the clearance range of interest. The cylinder nominal diameter was 2.00 in (5.08 cm) with clearance values, i.e., $\Delta r / r_i$, of 0.85×10^{-4}, 1.40×10^{-4}, 1.85×10^{-4}, 2.40×10^{-4}, and 3.40×10^{-4}, where r_i is the cylinder inner radius and Δr is the piston-cylinder clearance.

The spherical piston was installed on a tie-rod in the test fixture to permit adjustment of the piston within the cylinder. A pump in conjunction with an accumulator was used to supply hydraulic fluid to the test apparatus. The hydraulic fluid was filtered prior to entering the test apparatus to prevent foreign material from being trapped in the piston-cylinder annulus

Received February 21, 1975; revision received July 29, 1975. The author would like to acknowledge the assistance of B. L. McKamey and W. A. Bennett of the Research Dept., Detroit Diesel Allison Div., General Motors Corp., in carrying out the experimental investigations.

Index categories: Viscous Nonboundary-Layer Flows; Aircraft Subsystem Design.

*Center Fellow and Professor of Applied Mathematics. Associate Fellow AIAA.